Volume transition in composite poly(NIPAM)–giant unilamellar vesicles

Clément C. Campillo,[a] André P. Schröder,[b] Carlos M. Marques[b] and Brigitte Pépin-Donat*[a]

We have recently reported on the formation of composite gel vesicles prepared by the photopolymerization and crosslinking of poly(N-isopropyl-acrylamide) [poly(NIPAM)] inside phospholipid giant unilamellar vesicles (GUVs). Here we present a detailed study of the thermo-responsive behaviour of such composite vesicles. Giant vesicles filled with a poly(NIPAM) gel (gel–GUVs) exhibit a global volume phase transition, revealing a strong interaction between the gel and the phospholipid bilayer. Fluorescence studies show that the lipid membrane is not destroyed during the volume transition. The behaviour of giant vesicles filled with a poly(NIPAM) solution (sol–GUVs) depends on the volume fraction Φ_{NIPAM} of encapsulated NIPAM, the precursor monomer for poly(NIPAM). For $\Phi_{NIPAM} \leq 0.06$, we observe a frustrated demixing of the poly(NIPAM) chains in the internal medium; for $\Phi_{NIPAM} \geq 0.07$, sol–GUVs behave like homogeneous spheres and undergo a global volume phase transition similar to the one observed in gel–GUVs. For high volume fractions ($\Phi_{NIPAM} = 0.09$) achieved by osmotic deflation of low volume fraction ($\Phi_{NIPAM} = 0.03$) sol–GUVs, we observe a full demixing of the internal medium into two well-separated phases.

Introduction

Giant unilamellar vesicles or GUVs are micrometric capsules of phospholipid bilayers often used as simplified models of cell membranes.[1] In an effort to develop mechanico-mimetic systems of the whole cell, a number of biopolymers and other species have been added to the membrane[2–5] or encapsulated within the vesicle.[6–9] We have recently shown that GUVs filled with a gel of crosslinked poly(NIPAM) exhibit an elastic modulus comparable to that of living cells.[10] The elastic properties of these composite systems can be tuned by controlling the gel crosslinker content but also by exploiting the phase behaviour of poly(NIPAM). Indeed, poly(NIPAM) solutions exhibit lower critical solution temperature (LCST) behaviour, and the corresponding macroscopic poly(NIPAM) gels are known to decrease their volume as the temperature is increased from room temperature to around 32.5 °C.[11] For instance, for a polymer volume fraction of 0.13 and a crosslink ratio of 0.65, Hirokawa and Tanaka have shown that the volume of the gels smoothly decreases by a factor 2 in the range from 20 to 32.5 °C before suddenly collapsing by a factor of 5 at 32.5 °C. Above this temperature, the volume of the gel remains constant.

In previous studies,[9,12] GUVs filled with a poly(NIPAM) gel were shown to also undergo a significant volume change around 32.5 °C. The deswelling ratio $\alpha = V/V_0$, where V_0 is the gel volume at room temperature and V the volume after collapse, was in good agreement with experiments on comparable macroscopic gels.[11] Furthermore, α was found to be independant of the vesicle size, revealing no effect of the confinement inside the vesicles.

This paper reports a detailed study of the responses of various types of composite vesicles to temperature changes, in particular when the LCST is crossed. Using optical and fluorescence microscopy, we first study the behaviour of the membrane during the volume transition for gel-filled vesicles. Then we explore the non trivial behaviour of vesicles enclosing poly(NIPAM) solutions as they are driven through the LCST. We control the poly(NIPAM) volume fraction either by choosing the initial NIPAM concentration or by further decreasing the volume of the vesicle through osmotic deflation.

Materials and methods

Chemicals for preparation of composite giant unilamellar vesicles

The gel precursor mixture (pre-gel) encapsulated by the vesicles is prepared from N-isopropyl-acrylamide (NIPAM, Acros Organics), N,N'-methylene-bis-acrylamide (MBA, Sigma-Aldrich) and 2,2-diethoxyacetophenone (DEAP, Acros Organics). The phospholipids used in this work are 1,2-dioleoyl-sn-glycero-3-phosphocholine (DOPC, 99%, Sigma-Aldrich) and fluorescent 1-oleoyl-2-{12-[(nitro-2-1,3-benzoxadiazol-4-yl)amino]-dodecanoyl}-sn-glycero-3-phosphocholine (NBDPC, 99%, Avanti Polar Lipids). Chloroform (Sigma-Aldrich), methanol (Normapur), sucrose (99%, Sigma-Aldrich), glucose (99%, Sigma-Aldrich) and all other reagents are of analytical grade. All compounds are used as received.

Preparation of the precursor mixtures

The pre-gel aqueous solution is made from 0.1 M sucrose, 0.3 M NIPAM (corresponding to a monomer volume fraction $\Phi_{NIPAM} = 0.03$), 4.85 mM of the initiator DEAP, and 9 mM of the crosslinker MBA, corresponding to a 3% molar fraction of the monomer content. The pre-sol solution is made from 0.1 M sucrose, 0.1, 0.3, 0.45, 0.6 or 0.7 M NIPAM, corresponding to

[a] Laboratoire Electronique Moléculaire Organique et Hybride/UMR 5819 SPrAM (CEA-CNRS-UJF)/INAC/CEA-GRENOBLE, 38054 GRENOBLE, CEDEX 9, France
[b] Institut Charles Sadron, Univ. Louis Pasteur, CNRS - UPR 22; 23, rue du Loess, BP 84047, 67034 Strasbourg Cedex 2 France

Φ_{NIPAM} = 0.01, 0.03, 0.045, 0.06 or 0.07 respectively, and 4.85 mM DEAP. Oxygen dissolved in the pre-gel and pre-sol solutions was removed by bubbling dry argon for 30 min before the experiments.

Fabrication of giant unilamellar vesicles enclosing pre-gel or pre-sol mixtures

Vesicles containing the compounds required for gel (or sol) polymerization are prepared using the well-known electro-formation technique.[13] Two metallic (ITO) glass plates are covered with 20 µL of 1 mg mL^{-1} lipid in chloroform solution, and then dried under primary vacuum for 3 h. The two plates are assembled by a Sigillum wax (Vitrex, Copenhagen, Denmark) spacer to form a closed chamber filled with the pre-gel (or sol) solutions. A 10 Hz and 1 V alternative electric field is applied over a few hours. The GUVs are then removed from the growth chamber and kept in the dark in an Eppendorf vial filled with Argon.

Formation of the gel and sol-filled giant unilamellar vesicles

The preparation of the gel and sol-filled giant unilamellar vesicles (gel–GUVs and sol–GUVs) follows closely the preparation method previously described.[9,10,12] All the steps leading to the gel (or sol) formation are performed under a controlled argon atmosphere inside a glove box. Irradiation with a UV-B irradiation lamp (Sunlight-Erythemal, Harvard Apparatus) is performed through a band pass filter (320 nm–400 nm) that prevents the fluorescent phospholipids becoming damaged. The solution holders are 1 mL glass containers resting on ice packs and covered with a quartz window. The measured optical power density below the quartz window is 19 µW cm^{-2}, as measured by a silicon photodiode LM2 with an ×1000 attenuator and coupled to a Field Master GS from Coherent.

Sol–GUVs are prepared by UV-irradiation of 1 mL of the raw pre-sol GUV dispersion directly transferred from the electroformation chamber. After the photopolymerization, the sol–GUVs freely move within a surrounding poly(NIPAM) solution. The dilution of this poly(NIPAM) solution is finally obtained by adding an iso-osmotic glucose solution to a small volume of the sol–GUV dispersion. In contrast, the same protocol cannot be used for the gel–GUV preparation since it is essential to avoid the crosslinking of the polymer surrounding the GUVs, otherwise the GUVs would be trapped in an external gel. To achieve gel–GUV preparation, we dilute 50 µL of the pre-gel GUV solution described above into 1 mL of a so-called "dilution solution" (similar to the pre-gel mixture but without the crosslinker and where sucrose is replaced by glucose, as glucose allows sedimentation of the vesicles and observation by phase contrast microscopy). UV-irradiation is immediately performed in order to minimize crosslinker migration outside the vesicles. With this protocol, the polymer inside the gel-GUVs is crosslinked while the surrounding solution remains fluid. All the samples are irradiated for 5 min, removed from the glass containers and stored at 4 °C.

Optical and fluorescence microscopy

We use an inverted microscope Nikon TE 200, with a 40× DIC objective, a 100 W mercury lamp (HBO 103W/2, OSRAM), a fluorescence block with filters EX 450–490 nm/BA 520 nm, and a dichroic mirror 505 nm. Pictures are recorded with a digital camera (Diagnostic Instruments NDIAG 1800) onto the hard disk of a personal computer, with a pixel depth of eight bits. Fluorescence acquisition conditions are optimized as described elsewhere.[10]

Fluorescence image analysis

The fluorescence intensity profiles shown in the results section are directly extracted from the fluorescence images by substracting the background contribution. The total emitted fluorescence F of a given vesicle is quantified by integration of its intensity profile. For all the observed vesicles, the intensity F varies as the square of the vesicle radius R, providing a value for $f = F/(4\pi R^2)$, the fluorescence intensity per unit membrane surface. The rate of fluorescence loss due to photobleaching is measured by following f versus time on several vesicles. Wherever necessary, f can then be corrected for photobleaching, for each irradiation time and vesicle size.

Results and discussion

1. Fate of the membrane during the volume transition of gel-filled GUVs

We show in Fig. 1a a bright field image of a gel–GUV at 20 °C, and in Fig. 1b the corresponding image of the same vesicle well above 32 °C. As expected for poly(NIPAM) gels, increasing the temperature above 32 °C results in a reduction of the volume. The measured value of the deswelling ratio $\alpha = 0.06$ is here the same as the one reported by Campillo et al.[12] for similar sytems; it implies a 16.6 fold increase in the polymer concentration inside the vesicle and a 6.5 fold decrease in the gel bead surface. Such a variation of the composite vesicle dimensions implies also an important rearrangement of the phospholipid bilayer. The vesicle displayed in Fig. 1 was prepared with a small fraction of fluorescent lipids, which allows the visualization of its membrane by fluorescence microscopy before (Fig. 1c) and after (Fig. 1d) the volume transition. As these figures show, the membrane does not appear to lose its continuity during collapse and closely follows the shape of the gel surface.

The colocalization of the membrane and the gel surface during the volume transition can be further confirmed by comparing the intensity profiles of both the bright field and the fluorescence images (see Fig. 1e and 1f). The upper bright field profiles measured along the vesicle diameter have typical shapes for a refractive index discontinuity from the surface of a sphere. The corresponding fluorescence profiles shown at the bottom of the figures correspond in both cases to that expected for a fluorophore distribution on a spherical surface (see Appendix).

The total fluorescence F_{init} emitted by the vesicle before and the total fluorescence F_{shrunk} emitted by the vesicle after the transition have been measured as explained in the Materials and methods section. We found for all vesicles studied—see Fig. 2— that within experimental error F remains constant throughout
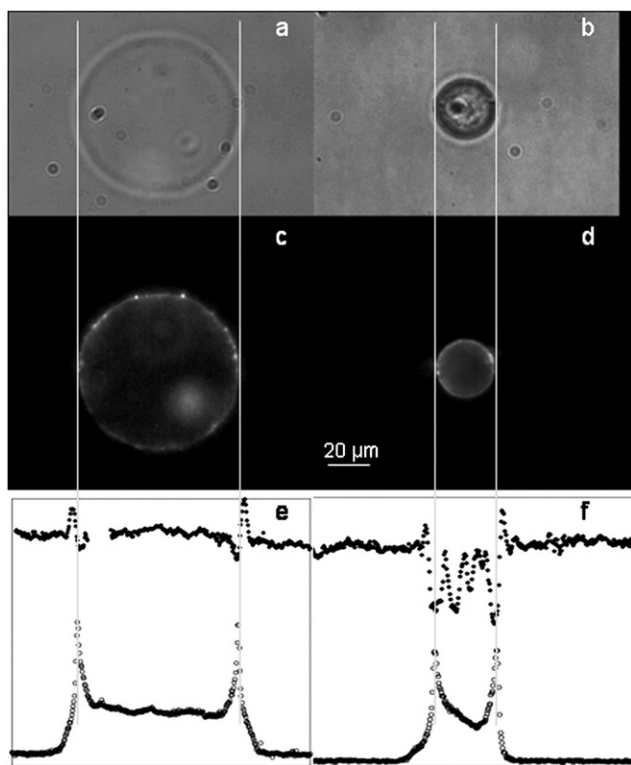
Fig. 1 Volume transition of a gel-filled vesicle. (a) Bright field image at room temperature and (b) above 32 °C. (c) Fluorescence image of the same vesicle at room temperature and (d) above 32 °C. (e) Bright field and fluorescence profiles along the diameter of the vesicle at room temperature and (f) above 32 °C.
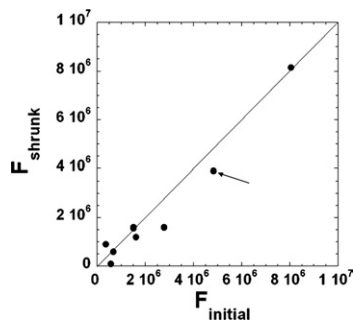
Fig. 2 Conservation of the total fluorescence during the phase transition as shown by the ratio between the initial fluorescence F_{init} and the fluorescence after transition F_{shrunk}.

the transition (notice that results shown in Fig. 1 correspond to the point indicated by an arrow in Fig. 2).

The experiments described in this section thus show that, within optical accuracy, the phospholipid membrane keeps its integrity and remains confined to the gel surface after gel collapse. Experiments not shown also revealed that the membrane recovers its initial shape and fluorescence distribution after the system has been cooled down to room temperature and the gel has recovered its initial volume. Although our results cannot reveal the membrane conformations at the suboptical

level, we speculate that the most likely pathway implies a reversible membrane crumpling during volume reduction.

2. Influence of the internal polymer concentration on the volume transition of sol-filled GUVs

Solutions of poly(NIPAM) also undergo a phase transition at 32 °C[14] resulting in a collapsed state of the polymer chains. At very low polymer volume fractions the chains collapse individually and can form microscopic aggregates responsible for the optical flickering of the solution. For higher concentrations, collective phase separation phenomena occur leading to a global volume transition.[15] We have followed the phase behaviour of poly(NIPAM) solutions confined in GUVs in the volume fraction range $0.03 < \Phi_{NIPAM} < 0.09$.

We show in Fig. 3 the behaviour upon heating of sol–GUVs prepared with different internal NIPAM volume fractions $\Phi_{NIPAM} = 0.03, 0.06, 0.07$ and 0.09. We stress that the differences in size are only due to the usual size dispersion of GUVs samples. Fig. 3 is separated in two parts: Fig. 3 row (a) shows sol–GUVs in their initial state, $T < 32$ °C. Fig. 3 row (b) shows the vesicles corresponding to those of row (a) when the temperature is increased over 32 °C. In Fig. 3 row (b), we observe local demixing of the poly(NIPAM) chains for the GUVs prepared with $\Phi_{NIPAM} = 0.03$ and 0.06, as has been already reported.[9,12,16] As expected, the internal medium of the vesicle flickers because of the concentration heterogeneities associated with the frustrated phase transition, but the radius of the vesicle remains constant. The behaviour observed in the case of the vesicle prepared with a volume fraction $\Phi_{NIPAM} = 0.07$ is dramatically different. The composite vesicle collapses as a whole, following thus a behaviour similar to vesicles enclosing crosslinked poly(NIPAM) gels. In order to check if the membrane collapses with the internal medium in vesicles prepared with $\Phi_{NIPAM} = 0.07$ as was demonstrated to be the case for gel–GUVs just before, we have labeled their membranes and observed them by fluorescence microscopy (Fig. 4). We notice that the membrane exhibits the same behaviour as in the case of gel–GUVs: the vesicle behaves like an homogeneous collapsing sphere.

As noticed above, collective phase separation phenomena in poly(NIPAM) solutions above a threshold polymer concentration have already been reported.[15] We confirmed this behaviour for a concentrated sample of a poly(NIPAM) solution ($\Phi_{NIPAM} = 0.15$): above 32 °C the solution separates into two distinct phases, *i.e.* a transparent one, and a second, optically dense, homogeneous phase, corresponding to a global demixing of the polymer chains (figure not shown). In the present case however this phenomenon is not observed in the sol–GUVs containing more than 7% of poly(NIPAM) (see Fig. 3). We indeed observe a collapse of the vesicle itself, similarly to gel–GUVs. This collapse cannot be attributed to an osmotic pressure drop upon increasing the temperature. Indeed, the contribution of the polymer chains to the osmotic pressure inside the vesicle is negligible. Therefore, we interpret this phenomenon as the result of a strong enough interaction between the polymer chains and the phospholipid membrane, so that the latter remains attached to the collapsing gel during the transition. Furthermore, the kinetic factors at play during the collapse must play an important role. For example, the life time of the chain entanglements has to
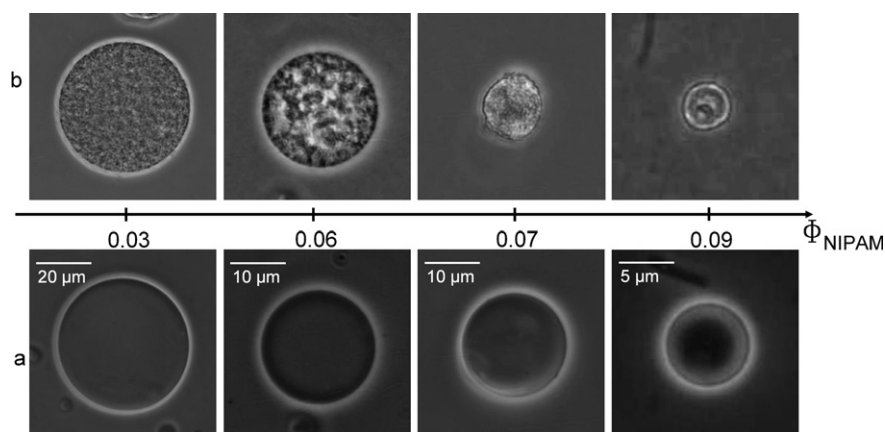
Fig. 3 The same series of sol–GUVs of various sizes prepared with $\Phi_{NIPAM} = 0.03$, 0.06, 0.07 and 0.09. Row (a) at $T<32$ °C. Row (b) when the temperature is increased at $T>32$ °C.
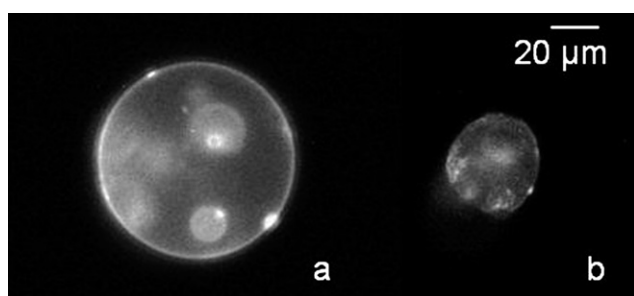
Fig. 4 Sol–GUV ($\Phi_{NIPAM} = 0.07$): (a) at $T<32$ °C and (b) $T>32$ °C observed in fluorescence revealing the collapse of the membrane with the internal medium. Heterogeneities (here observed) are often present on GUVs prepared this way, and not taken into account in this study.

Fig. 5 Phase transition of a sol–GUV as a function of its deflation degree, as obtained from osmotic pressure increase. (a) The vesicle in the initial state (non deflated, $\Phi_{NIPAM} = 0.03$) at room temperature, (d) the vesicle after the thermal transition; (b) the same vesicle deflated to $\Phi_{NIPAM} = 0.06$ at room temperature and then (e) after the thermal transition; (c) the same vesicle deflated to $\Phi_{NIPAM} = 0.09$ at room temperature and observed (f) after the thermal transition; (g) time series of the thermal transition between the initial state shown in (c) and the final state in (f) (at $t = 0$, the temperature is raised to 32 °C).

be greater than the duration of the thermal transition, so that the polymer chains attached to the membrane remain entangled with the internal solution during the whole process. Also, an important role must be played by the nature of the polymer–membrane interaction. For instance, if the interaction is not of a covalent nature, then the lifetime of the chain–membrane bond must be greater than the duration of the thermal transition. We will see in the following section that under some conditions, sol–GUVs containing a concentrated poly(NIPAM) solution can exhibit a different kind of collapse than the one described here.

3. Osmotic pressure control of the volume transition in sol-filled GUVs

The polymer volume fraction of a single sol-GUV can also be controlled by driving the external osmotic pressure, thereby providing a precise control of the vesicle's response to temperature as shown in Fig. 5.

We started with a vesicle initially at room temperature and Φ_{NIPAM} equal to 0.03 (Fig. 5a). The vesicle was then submitted to two successive heating–cooling–deflating cycles, as described below. The first heating cycle confirms what has been observed previously: for the low polymer volume fractions ($\Phi_{NIPAM} = 0.03$), the transition leads to a flickering of the internal medium of the vesicle (Fig. 5a and 5d), which is attributed to a frustrated,

local demixing of the inner solution. After cooling the sol–GUV back to room temperature, the osmotic pressure of the outer solution is increased to induce a 50% decrease of the total volume of the vesicle, leading to an inner polymer volume fraction of $\Phi_{NIPAM} = 0.06$ (Fig. 5b). The heating of the overall system above 32 °C leads again to a local demixing of the inner solution, with a qualitatively similar result to that described in Fig. 3a and 3b (flickering of the internal medium). After cooling back to room temperature, a second deflation is imposed to the vesicle by increasing the osmotic pressure, that leads to a new reduction of the vesicle volume, corresponding to a polymer volume fraction of $\Phi_{NIPAM} = 0.09$ (Fig. 5c). The following heating cycle leads to a non expected behaviour of the inner solution, as seen in Fig. 5f. The transition causes in this case a macroscopic phase separation, the kinetics of which is shown in Fig. 5g.

Coming back to the deflation phases corresponding to Fig. 5b and 5c, it is likewise worthwhile noting that the vesicle ejects small daughter vesicles and membrane tethers. This mechanism allows the vesicle to remain spherical. Furthermore, we do not
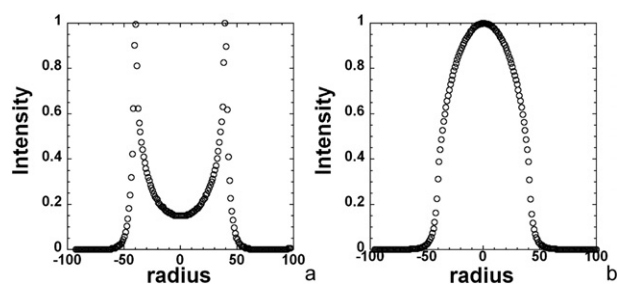
Fig. 6 Simulated fluorescence intensity profiles for a vesicle with fluorescent membrane (a) and a vesicle filled with fluorescent solution (b).

observe any flickering of the daughter vesicles at the phase transition (Fig. 5e and 5f), revealing that these vesicles do not contain a noticeable quantity of poly(NIPAM). Thus the poly(NIPAM) amount in the mother vesicle is assumed to be constant, and the above calculated concentrations of 6% and 9% should hold.

Fig. 5g illustrates the kinetics of the thermal transition from $T<32$ °C (Fig. 5c) to $T>32$ °C (Fig. 5f). At $t = 0$, the temperature is suddenly raised to 32 °C. The phase separation of the poly(NIPAM) and water solution inside the vesicle increases as the time elapses. Eventually two distinct fluid phases form (Fig. 5f) consisting of a hydrophobic poly(NIPAM) phase and a hydrophilic phase. Because such deflated vesicles exhibit a dynamic phase separation, they are good candidates to mimic the process of microcompartmentation during cellular activity.[17,18]

It might seem surprising to observe two distinct behaviours for GUVs enclosing similar poly(NIPAM) solutions (similar Φ_{NIPAM}) as observed in Fig. 3 and 5 for $\Phi_{\mathrm{NIPAM}} = 0.09$. However, these two experiments differ because in one case $\Phi_{\mathrm{NIPAM}} = 0.09$ is fixed at the preparation stage (Fig. 3) while in the other case, the initial Φ_{NIPAM} is low and the final $\Phi_{\mathrm{NIPAM}} = 0.09$ is obtained by deflation (Fig. 5). Although both types of vesicles share the same final Φ_{NIPAM}, the structure of these two kinds of GUVs should differ because the polymerization of their internal media was performed at different NIPAM concentrations. This difference changes presumably (i) the polymer molecular mass, and therefore the entanglement lifetimes evoked above, and (ii) the membrane–poly(NIPAM) interactions.

Conclusions

In this paper we show that composite GUVs encapsulating poly(NIPAM) covalent gels collapse and behave like homogeneous spheres when the temperature is increased above that of the poly(NIPAM) transition; their membrane remains undamaged at the optical resolution and sticks to the internal gel during its collapse.

Furthermore, we also show that composite GUVs encapsulating poly(NIPAM) sol exhibit three distinct behaviours during the poly(NIPAM) transition. At low poly(NIPAM) volume fraction ($\Phi_{\mathrm{NIPAM}}\leq0.06$), the membrane of the composite sol–GUVs remains unchanged. Their internal medium exhibits a local submicrometre-scale phase separation with visible density fluctuations, while the vesicle remains unchanged in size. When these vesicles are deflated above a threshold volume fraction

(for example $\Phi_{\mathrm{NIPAM}} = 0.09$ starting from an initial $\Phi_{\mathrm{NIPAM}} = 0.03$), their internal medium exhibits a macroscopic two-phase partitioning. For vesicles prepared with a higher poly(NIPAM) volume fraction ($\Phi_{\mathrm{NIPAM}}\geq0.07$) at the preparation stage (*i.e.* from the polymerization of a monomer solution of the same concentration), the composite GUVs behave like homogeneous spheres collapsing as a whole.

At this point, one may list the various potential applications of these thermo-responsive bio-compatible systems. Those vesicles could be used *in vivo* as thermo-responsive drug carriers. Their membranes could be covered with adhesive molecules to target a specific organ and liberate encapsulated drugs in response to temperature changes. Such systems also hold promise as good mechanically responsive systems with the potential to mimic cellular motility. In addition, this type of composite vesicle may be regarded as a first step to achieve sophisticated multi-phase cell models that are able to mimic nucleated cells.

Appendix

The observed image $I(x,y,0)$ in the focal plane is the convolution product[19] of the object image $O(x,y,z)$ and the point spread function of the microscope (PSF), $I(x,y,0) = \int dx' dy' dz' \, \mathrm{PSF}(x - x', y - y', 0 - z') O(x', y', z')$. The PSF has been experimentally determined for our observation conditions by scanning the function $I(x,y,z)$ for a dot like fluorescent object, typically a fluorescent bead of suboptical size: $I(x,y,z) = \int dx' dy' dz' \, \mathrm{PSF}(x - x', y - y', z - z') \delta(x', y', z') = \mathrm{PSF}(x,y,z)$. We simulated the microscope PSF using the public domain imaging software ImageJ. The parameters in the software were chosen such that they provided a good agreement between the experimental and the simulated PSF. The simulated PSF was then convoluted with a tridimensional representation of the vesicles $O(x,y,z)$.

For the sake of distinguishing fluorescent profiles for vesicles with membrane bound fluorophores and vesicles with a bulk density of fluorophores, we consider two very different cases. First a hollow sphere whose surface is fluorescent and second a sphere full of fluorophores. In the first case of a fluorescent membrane, we obtain the fluorescence profile displayed on Fig. 6a, in the second case of a full sphere, the profile is shown in Fig. 6b. Comparison of Fig. 6a and profile characteristics of the vesicles studied in this paper (see Fig. 1e and 1f) shows that in all cases the membrane remains confined at the surface of the composite vesicles.

References

1 R. Lipowsky and E. Sackmann, *Structure and dynamics of Membranes*, Elsevier, 1995.
2 V. Frette, I. Tsafrir, M. Guedeau-Boudeville, L. Jullien, D. Kandel and J. Stavans, *Phys. Rev. Lett.*, 1999, **83**, 2465.
3 F. Quemeneur, A. Rammal, M. Rinaudo and B. Pépin-Donat, *Biomacromolecules*, 2007, **8**, 2512–2519.

4 O. Mertins, M. B. Cardoso, A. R. Pohlmann and N. P. Silveira, *J. Nanosci. Nanotechnol.*, 2006, **6**, 2425–2431.

5 H. Ringsdorf, E. Sackmann, J. Simon and F. Winnik, *Biochim. Biophys. Acta*, 1993, **1153**, 335–344.

6 O. Stauch, T. Uhlmann, M. Fröhlich, R. Thomann, M. El-Badry, Y.-K. Kim and R. Schubert, *Biomacromolecules*, 2002, **3**, 324–332.

7 A. Viallat, J. Dalous and M. Abkarian, *Biophys. J.*, 2004, **86**, 2179–2187.

8 L. Limozin and E. Sackmann, *Phys. Rev. Lett.*, 2002, **89**(16), 168103.

9 M. Faivre, C. Campillo, B. Pépin-Donat and A. Viallat, *Prog. Colloid Polym. Sci.*, 2006, **133**, 41–44.

10 C. Campillo, A. P. Schröder, C. M. Marques and B. Pépin-Donat, *Mater. Sci. Eng., C*, submitted.

11 Y. Hirokawa and T. Tanaka, *J. Chem. Phys.*, 1984, **81**(12), 6379.

12 C. Campillo, B. Pépin-Donat and A. Viallat, *Soft Matter*, 2007, **3**, 1421.

13 M. I. Angelova and D. S. Dimitrov, *Faraday Discuss. Chem. Soc.*, 1986, **81**, 303–311; M. I. Angelova and D. S. Dimitrov, *Faraday Discuss. Chem. Soc.*, 1986, **81**, 345–349.

14 H. Schild, *Prog. Polym. Sci.*, 1992, **17**, 163–249.

15 F. Zeng, X. Zheng and Z. Tong, *Polymer*, 1998, **39**(5), 1249–1251.

16 A. Jesorka, M. Markström and O. Orwar, *Langmuir*, 2005, **21**(4), 1230–1237.

17 M. Helfrich, L. Mangeney-Slavin, M. Scott-Long, K. Djoko and C. Keating, *J. Am. Chem. Soc.*, 2002, **124**, 13374–13375.

18 M. Scott-Long, C. Jones, M. Helfrich, L. Mangeney-Slavin and C. Keating, *Proc. Natl. Acad. Sci. U. S. A.*, 2005, **102**(17), 5920–5925.

19 B. Herman and H. J. Tanke *Fluorescence Microscopy*, Springer, 1998.